Transient Response of Ventilated Room Enclosure Subjected to Solar Radiation Load

Lect. Mustafa Ahmed Abdulhussain
mustafa.ahmed1971@gmail.com
University of Technology - Mechanical Engineering Dept.

Abstract

The effect of incident solar radiation ray's penetration through glassed windows of duct - ventilated room enclosure air is investigated assuming constant solar intensity. The room is supplied with cold dry air through rectangular duct and the air is distributed through two grid ceiling fans located at the duct exit. The effect of fixed solar intensity penetration with variable fans rotational speed at specified time intervals is investigated upon the room temperature distribution and is simulated using the ANSYS CFX package. The results showed the variation in room temperature distribution at a specified time period (1, 2, 3 minutes) with increased fan speed becomes more efficient, also the transient room temperature distribution response to the solar radiation is significantly present in the simulation noticing fans effect on accelerating heat transfer rate through the domain.

Keywords: Ventilated room, ceiling grid fans, solar radiation.

Introduction

The new design feature of ceiling fans with twin rotating technique have better improved ventilation over the old past ones.

This design gives more efficient air circulation across the space enclosed. Its operating principle as shown in figure (1) is to draw air from the four-sided meshed entrance and blow it via the fan blades and the rotating meshed disk. This technique can be multi-installed around the space.

J. Fan et al. (2013) have studied the performance analysis of the new designed ventilation in an office room experimentally and numerically. They studied the variation in room temperature, air speed, the wall temperature and pressure as well as the ventilation effectiveness, they concluded the ventilation flow mixing is quite good above the occupied zone and the ventilated flow rate is insignificant effect on the ventilation effectiveness.

A. El Degwy and E. Khalil (2017) simulated the ordinary 5-blades ceiling fan room ventilation by the CFD FLUENT package, they studied achieving the best occupant comfort conditions by changing the blades twist angle and the fan speed, the results showed that lower blades twist angles are suitable for the low height rooms and vice versa.

A novel room ventilation system integrated solar ceiling effect was adopted by **C. Zhang et al (2017)** that provides energy efficient and occupant comfort conditions, the model involved diffusion of ventilated ceiling air in a plenum that is sub cooled via water piping incorporated into radiant ceiling . Several ceilings design parameters have been investigated such as diffused ceiling configuration, plenum geometry, shape and location of the plenum inlet, they tested the numerical simulation experimentally. The results showed that the diffuse ceiling increases the heating capacity of the radiant ceiling but decreased its cooling capacity, meanwhile the diffused ceiling panel overall heat transfer coefficient higher value will increase the radiant ceiling cooling efficiency. In addition, the low height plenum enabled forced convection between supply air and radiant ceiling, and enhanced the energy efficiency of the system. However, the reduction in plenum height deteriorated the uniformity of air distribution

through the diffuse ceiling and resulted in a higher draught in the occupied zone.

The solar radiation intensity in IRAQ middle and south regions **(F. H. Mahmood and G. S. Al-Hassany, 2014)** is considerably high during summer term (May, June, July and August) leading to severe draft hot weather conditions (exceeds 50 °C in July and August). Also, the relatively high thermal - conducted building materials with highly solar radiation absorbing and penetration capability frequent using have adversely affected the comfort living conditions and also the healthy good supplies storage.

Double Glazed windows room temperature distribution with solar film coating layer have been simulated numerically by **J. Xaman et al. (2016)** in hot and cold weather climate conditions, the model consisted of two glazed window layers with circulated air between them, the solar film layer is attached at internal glazed window for cold climate condition, at external window for hot condition. They concluded that the solar film usage would reduce the room enclosure heat gain by (62%) for warm environment, at cold weather conditions, the solar film layer effect is considered negligible remarking similar room temperature distribution with non- utilizing coating layer.

One of the most frequently used solar radiation CFD models is the Monte Carlo path tracing approach. **M. Popvac et al. (2010)** modeled the solar radiation rays as released beams from fixed position that passes and interacts with non-ventilated room enclouser taking into account the absorption, reflection and refraction phenomenon with heat exchange with surrounding surfaces. The Monte Carlo CFD approach gave diminished solution obstacles for simple and complex room's geometries, and reduce computational hardware overloading. The solar radiation walls acts as heating source for the inner field walls and the natural convection criteria is the dominant effect for heating the flow field.

S. Gendelis, and A. Jakovics (2008) simulated the incident solar radiation heating effect on a room enclosure with ventilation opening by the ANSYS-CFX package, taking into consideration the solar penetration through the windows as a heating source with constant intensity and different incident angle then the air enclosed is heated through natural convection. The solar incident angle below 45°C gives increased heating effect because of the deeper ray's penetration.

Cold air room ventilation cfd simulation effectiveness parameters have been studied by **A. Yousef et al. (2017)** considering different air supply conditions with enclosed variable subjected thermal loads, the comfort condition level was detected through calculation of the air diffusion performance index (ADPI). The most important conclusion is the supply cold air reduced velocity and temperature does not affect the comfort level and improved the ADPI.

The aim of the present paper is to investigate the grid ceiling fan suction-blow modification by CFD-simulation. The modification is performed by changing the flow intake through the axial direction (not circumferentially). This will lead to multi blow directions (axially and circumferentially).

A ventilated duct supplies cold air to the room enclosure is distributed via two ceiling fans with polypropylene material. The room contains two typical glass windows subjected to direct solar radiation; the room contains one opening for flow exit. The simulation was modeled in the ANSYS CFX assuming transient flow conditions at specified time intervals (1, 2 and 5 minutes). The radiation density is considered constant (due to short time simulation), also variable fan velocity is conjugated in the work assuming room and duct walls are insulated. The standard K-ε turbulence model was utilized in the simulation.

The geometry building

The duct – ventilated room basic geometry as shown in figure (2a) including the ceiling fans is built using SOLIDWORKS

2016. The room dimensions are (4.7*3.0) with 2.5 m height with two windows and one opening. The duct has a rectangular shape of (0.6*0.2 m) cross section divided into two branches where the fans are located. The fans structure is a square shaped of (60 cm) length and (10 cm) thickness with one inlet and five exits (four fixed circumferential opening and one rotating disk exit).

The CFD modelling

1. Numerical solution technique

The CFX package demonstrates the finite volume approach in which the governing Navier-stokes equations (1), the energy (2) and the turbulence model equations (3) are integrated around the mesh elements.

$$\rho\left(u\frac{\partial u}{\partial x}+v\frac{\partial u}{\partial y}+w\frac{\partial u}{\partial z}\right)=X-\frac{\partial P}{\partial x}+\mu\left(\frac{\partial^2 u}{\partial x^2}+\frac{\partial^2 u}{\partial y^2}+\frac{\partial^2 u}{\partial z^2}\right)$$

$$\rho\left(u\frac{\partial v}{\partial x}+v\frac{\partial v}{\partial y}+w\frac{\partial v}{\partial z}\right)=Y-\frac{\partial P}{\partial y}+\mu\left(\frac{\partial^2 v}{\partial x^2}+\frac{\partial^2 v}{\partial y^2}+\frac{\partial^2 v}{\partial z^2}\right)$$

$$\rho\left(u\frac{\partial w}{\partial x}+v\frac{\partial w}{\partial y}+w\frac{\partial w}{\partial z}\right)=Z-\frac{\partial P}{\partial y}+\mu\left(\frac{\partial^2 w}{\partial x^2}+\frac{\partial^2 w}{\partial y^2}+\frac{\partial^2 w}{\partial z^2}\right)$$

……..(1)

$$\rho C_p\left(u\frac{\partial T}{\partial x}+v\frac{\partial T}{\partial y}+w\frac{\partial T}{\partial z}\right)=k\left(\frac{\partial^2 T}{\partial x^2}+\frac{\partial^2 T}{\partial y^2}+\frac{\partial^2 T}{\partial z^2}\right)+\mu\Phi$$

where

$$\Phi=\left[2\left(\frac{\partial u}{\partial x}\right)^2+2\left(\frac{\partial v}{\partial y}\right)^2+2\left(\frac{\partial w}{\partial z}\right)^2+\left(\frac{\partial u}{\partial y}+\frac{\partial v}{\partial x}\right)^2+\left(\frac{\partial u}{\partial z}+\frac{\partial w}{\partial x}\right)^2+\left(\frac{\partial v}{\partial z}+\frac{\partial w}{\partial y}\right)^2\right]$$

…….. (2)

2. The turbulence modeling

The standard scalable K-ε model is utilized in the problem analysis with empirical equations constants.

$$\frac{\partial(\rho k)}{\partial t}+\nabla.(\rho \boldsymbol{U}\, \mathrm{k})=\nabla.\left[\left(\mu+\frac{\mu_t}{\sigma_k}\right)\nabla k\right]+P_k-\rho\varepsilon$$

$$\frac{\partial(\rho \varepsilon)}{\partial t}+\nabla.(\rho \boldsymbol{U}\, \varepsilon)=\nabla.\left[\left(\mu+\frac{\mu_t}{\sigma_\varepsilon}\right)\nabla \varepsilon\right]+\frac{\varepsilon}{k}\left(C_1 P_k-C_2\rho\varepsilon\right) \quad \ldots\ldots\ldots (3)$$

Where, $C_{1=}$ 1.42, C_2= 1.68, $\sigma_k = \sigma_\varepsilon$ = 0.72 [2].

The problem involved modeling of translational and rotational flow domains (including stationary and rotating meshing treatment) where the rotating domains includes the fan blades flow region and the rotating fan disk Also, the interference between higher momentum fan-circulating flows with room still-air has considered as a matter of great importance in the transient flow analysis.

3. Geometry meshing

The room enclosed with supplied duct ventilation were meshed using the standard tetrahedrons meshing technique shown in figure (2b) with hided walls and windows , the mesh consisted of more than (325000) nodes and (1750000) elements taking the minimum and maximum mesh elements sizes by their default values of (2.8e-3) and (0.56) meters with (1.2 growth rate) concentrated at the rotational flow domain, slow transition solution procedure among nodes and cells has been adopted taking the curvature coarse sizing function.

4. Solar radiation modeling

In CFX, radiation is treated as photons rays tracked by the flow domain using the following spectrum travel equation

$$\frac{dIv(r,s)}{ds} = -(Kav + Ksv).Iv(r,s) + Kav.Ib(v,T) +$$

$$\frac{Ksv}{4\pi}\int dIv(r,s).\varphi.(s,s).d\omega + S \qquad \ldots\ldots\ldots (4)$$

The most appropriate solar model suggested by S. **Gendelis, and A. Jakovics (2008)** is the Monte-Carlo model that consider the rays as photon gas released from its source is tracked through the domain until it falls at a surface where several phenomena occurs every time step like scattering, diffusing or absorption depending on the rays - targeted surface and domain composition. A tracking data of the photon is developed in the CFX modeling, the photons are considered a participating media with non-scattering occurrence.

5. Setting the boundary conditions

The duct air velocity is assumed uniform of (15 m/s) with temperature (10°C), while room still-air initial temperature of (25°C), glass windows are assumed constant temperature of (45°C). The flow is assumed to be at atmospheric pressure conditions with neglecting heat transfer through walls, flour and ceiling (adiabatic with no slipping flow walls). Overall heat transfer for the room flow enclosure with glass windows is taken (2.5W/m^{2}K) [7].

6. Solving initializing

Taking into consideration the gravity effect, the flow gravity acceleration has been activated; flow initialization values were taken close to the appointed boundary conditions. The solution basic setting has been taken as high resolution equations advection scheme with transient second order backward Euler method, the convergence limit was set to (1e-4). Taking fans rotational velocity of both (100 and 500 rpm) respectively, the model is simulated at transient time intervals of (1, 2, and 5 min) with constant time step of (1 sec) for each run.

Results and discussion

1. Air circulation

Figures (3-10) demonstrates the flow field velocity vectors and circulation contours in the room at 3 different planes locations (mid room length, mid-width and beneath the fans directly) where the flow is distributed circumferentially in four directions and axially through the meshed disk, In figures (3 &4) the fan blades operation increased flow turbulence and mean velocity vector distribution circumferentially rather than the axial disk does remarking slightly increased flow velocity vector due to fan higher rotation and also the fan case makes significant reduced velocity magnitudes. The transient response of increased fan velocity as observed in figures (5-10) shows the gradual flow field acceleration for the enclosed space and the rapid flow circulation though and surrounding the fans noticing increased circulation near the side room walls.
Figure (10) represents the iso-planed surface circulated flow pattern located at mid-fan body shows the locally increased velocity contours.

2. Solar heating effect

Figures (11-14) represents the entire flow heating due to solar radiation effect. Figures (11&12) indicates the time step transient heating effect on ceiling and duct flow, although the duct and the walls are insulated, the circulated flow contribute in improved cooled space especially for higher flow turbulence as shown in figures (13&14).

One of the important remarks that have been concluded from the temperature contours in figures (15&16) is the increased speed circulated air especially at the windows side noticing local sub cooled circulated air region above the windows side vanishes gradually with fans speeding, also figures (17&18) clears the time dependent increased heating effect especially above and in the windows level. The gradual duct flow heating

is caused by the fan fixed structure accumulated heat absorbed. The room enclosed temperature distribution in figure (19) shows the heating effect of the limited incident solar radiation due to short simulation time period.

References

[1] J. Fan, C. A. Hviid, and H. Yang "Performance analysis of a new design of office diffuse ceiling ventilation system", Energy and Buildings, Vol.59, pp: 73–81, (2013).

[2] A. El Degwy and E. E. Khalil," Simulation of air flow pattern in a room with ceiling mounted circulator", 55th AIAA Aerospace Sciences Meeting, 9 - 13 January 2017.

[3] C. Zhang, P. K. Heiselberg, Q. Chen and M. Pomianowski, "Numerical analysis of diffuse ceiling ventilation and its integration with a radiant ceiling system", Building Simulation, Vol.10, Iss.5, pp:203-218, 2017.

[4] F. H. Mahmood, and G. S. Al-Hassany," Study Global Solar Radiation Based on Sunshine Hours in Iraq", Iraqi Journal of Science, Vol. 55, No.4a, pp: 1663-1674, 2014.

[5] J. Xamán, Y. Olazo-Gómez, G. Álvarez, I. Hernández-Pérez, J.O. Aguilar and J.F. Hinojosa," Thermal Evaluation of a Room coupled with a Double-Glazing Window with/without a Solar Control Film for Mexico", Applied Thermal Engineering, Vol.110, Iss.1, pp: 805-820, 2017.

[6] M. Popovac, B. Kubicek, A. Frohner and B. Semlitsch, "Path-tracing Approach for Solar Radiation Modeling in CFD", International Solar Energy Society Conference Proceedings, 2010.

[7] S. Gendelis and A. Jakovics," Mathematical modelling of a living-room with a solar radiation source and different boundary conditions", heat & power and thermal Physics, Vol.1, pp: 73-83, 2008.

[8] A. A. Youssef, E. M. Mina, A.R. El Baz, and R.N. Abdel Messih, "Studying comfort in a room with cold air system using computational fluid dynamics" Ain Shams Engineering Journal, 2017.

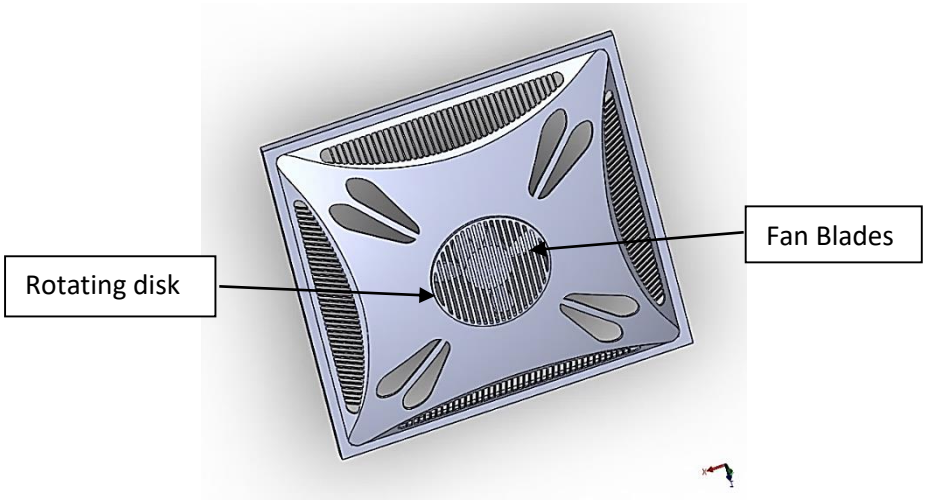

Figure (1) Ceiling wall grid fan

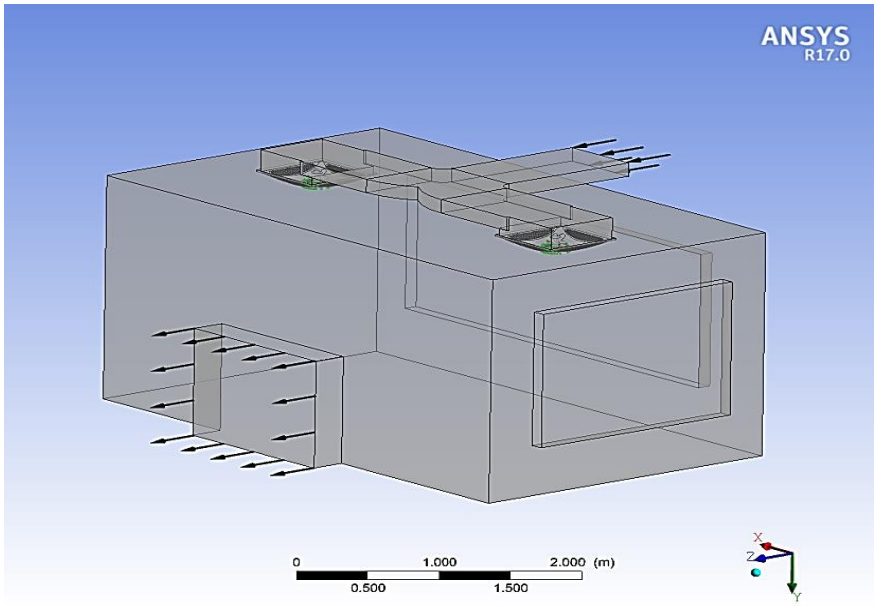

Figure (2a) Geometry description

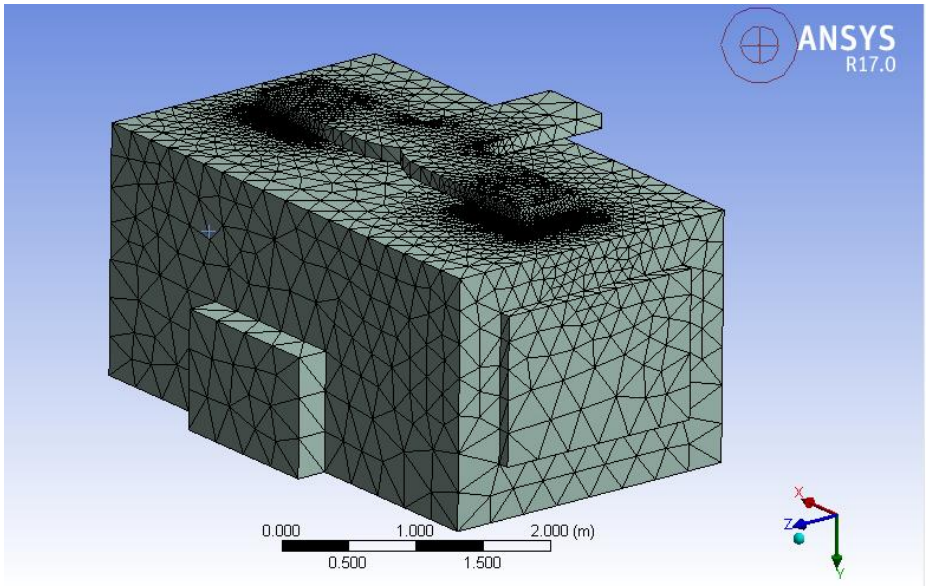

Figure (2b) geometry meshing

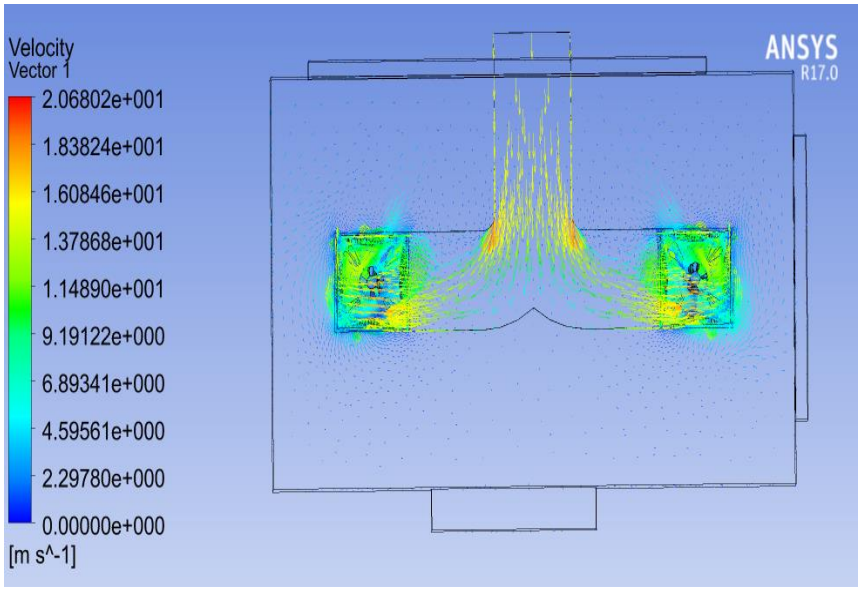

Figure (3) the flow field velocity vector for the entire room enclosure at t=2 min with Ω=500 RPM

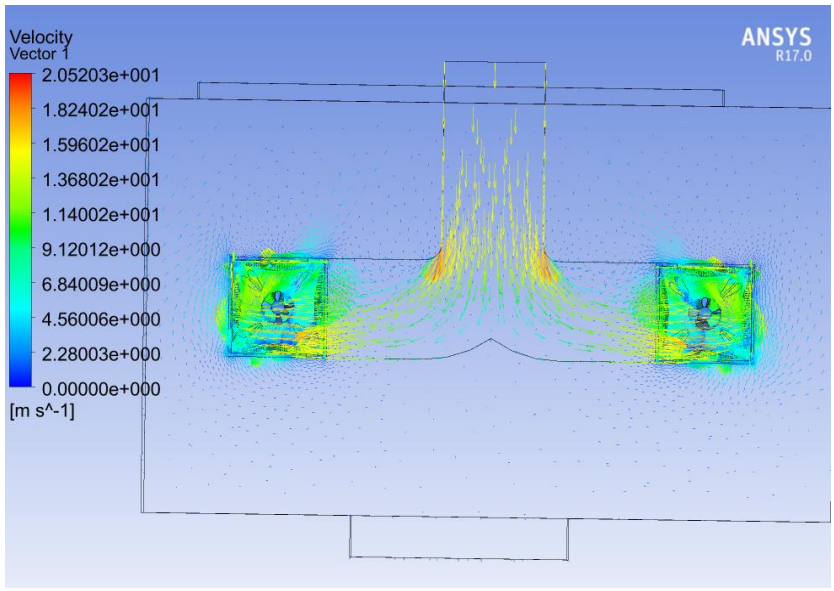

Figure (4) the flow field velocity vector for the entire room enclosure t=2 min with Ω=100 RPM

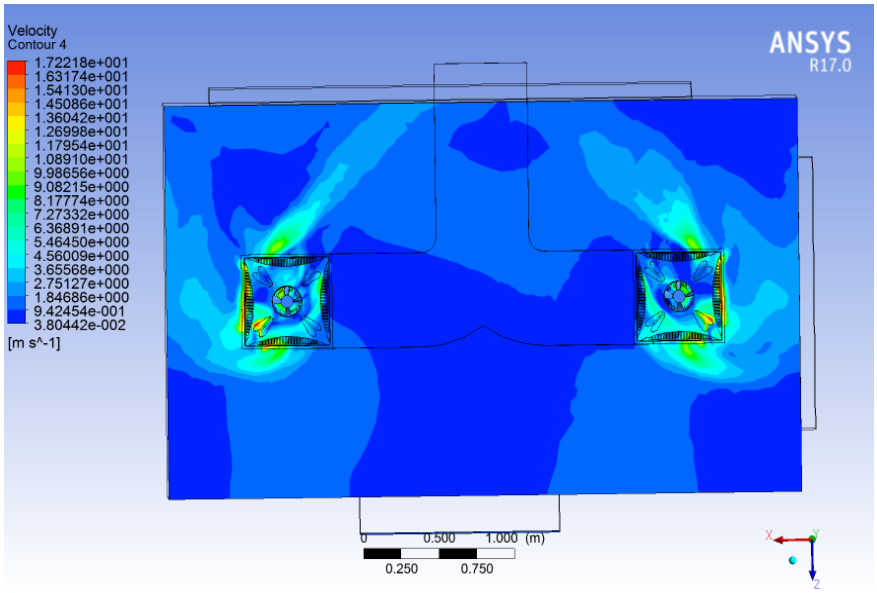

Figure (5) the flow field circulation beneath the fans directly at t=1 min with Ω=100 RPM

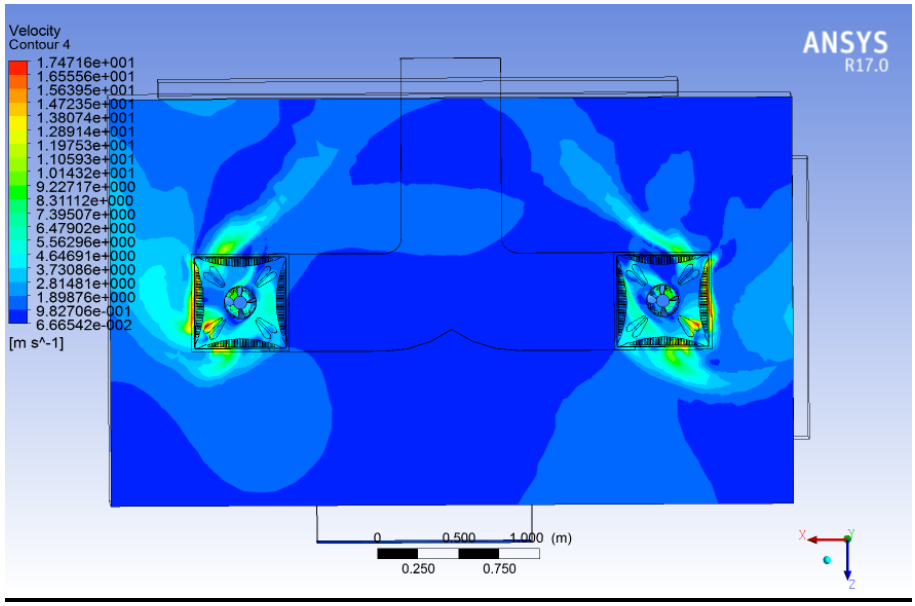

Figure (6) the flow field circulation beneath the fans directly at t=2 min with Ω=100 RPM

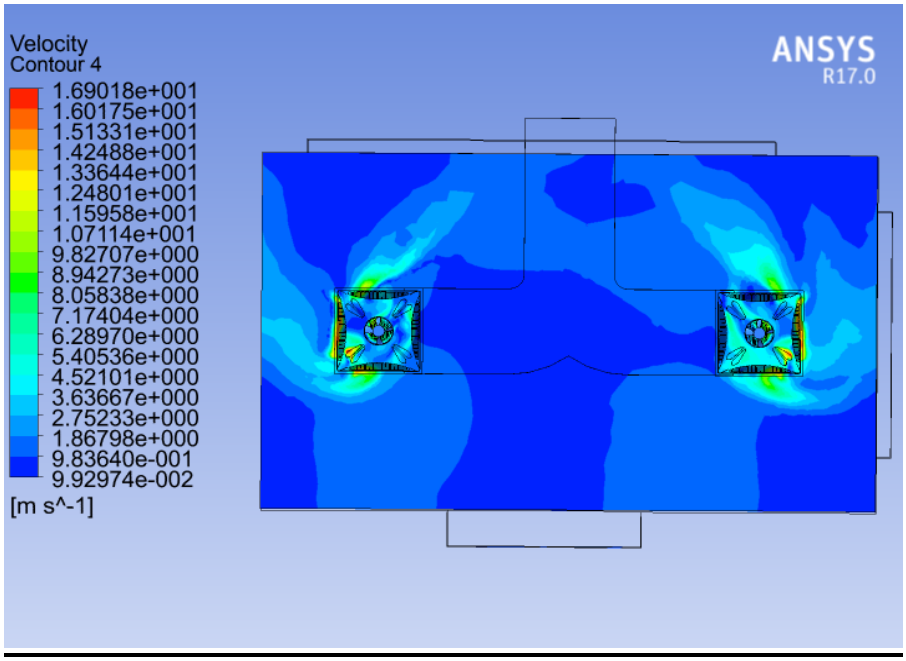

Figure (7) the flow field circulation beneath the fans directly at t=5 min with Ω=100 RPM

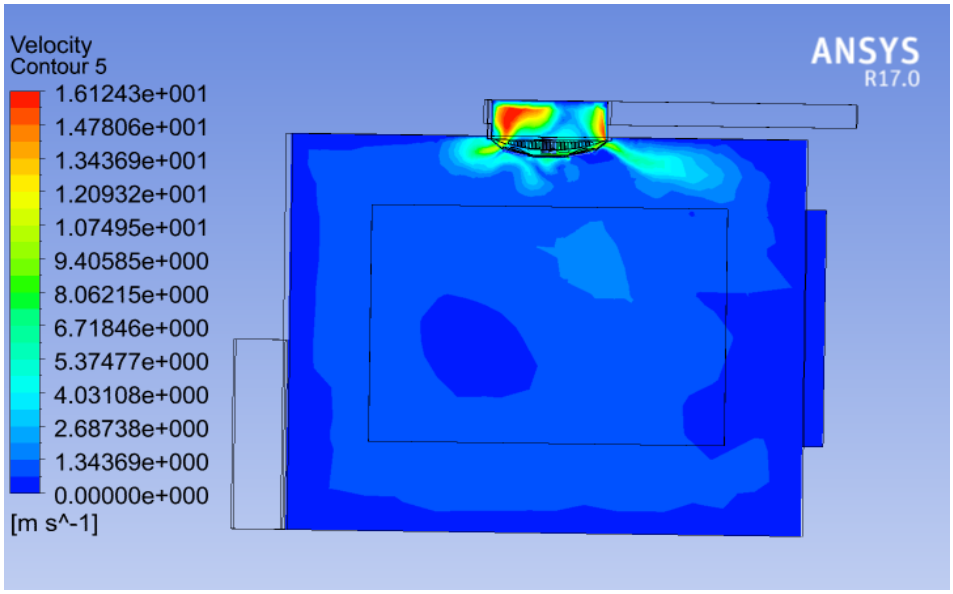

Figure (8) the flow field circulation in fan section at t=1min with Ω=100 RPM

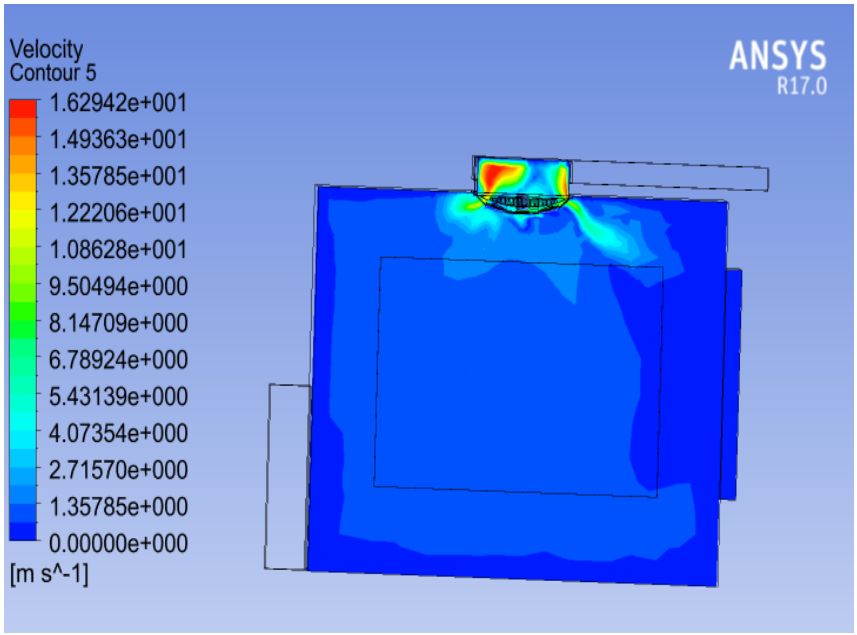

Figure (9) the flow field circulation in fan section at t=2min with Ω=100 RPM

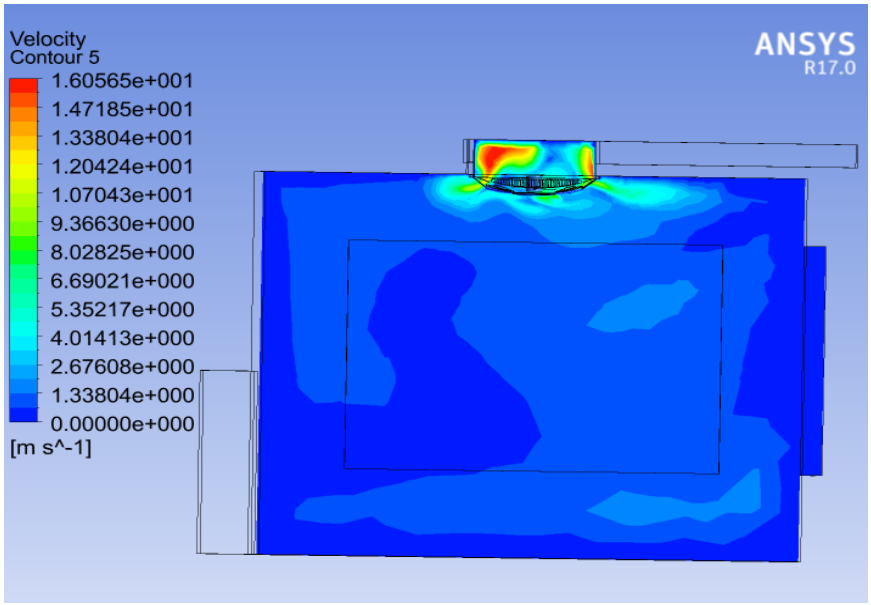

Figure (10) the flow field circulation in fan section at t=5min with Ω=100 RPM

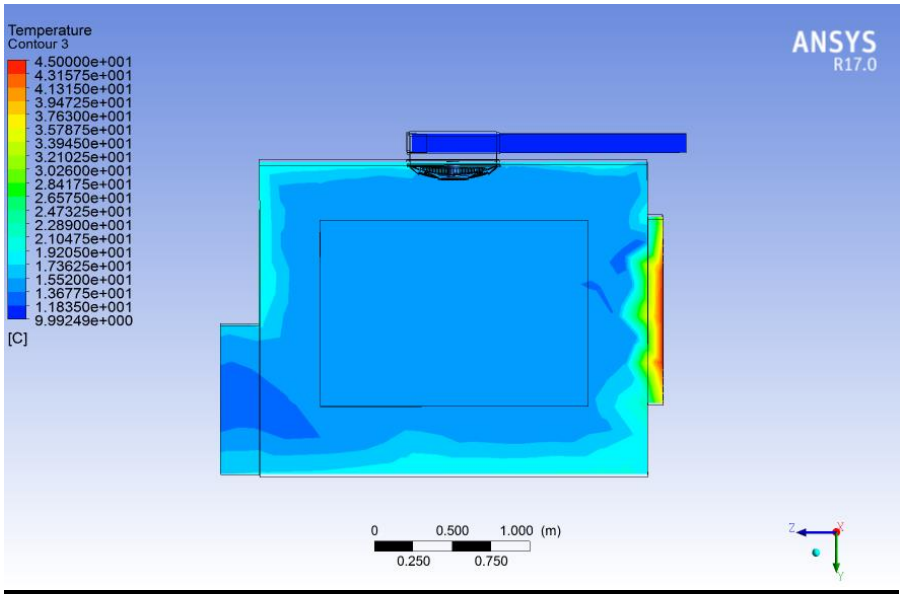

Figure (11) the flow temperature distribution at t=1 min with Ω=100 RPM in room-mid width

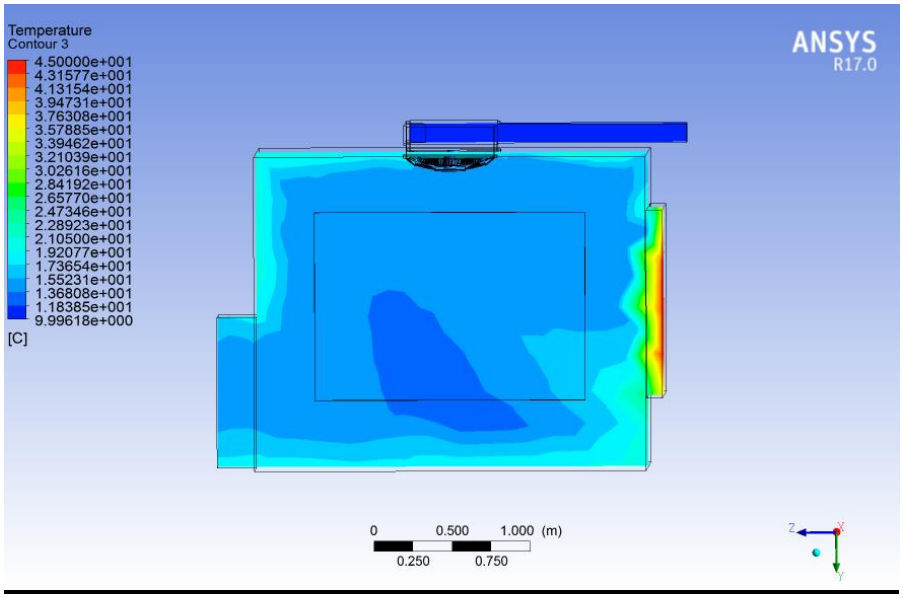

Figure (12) the flow temperature distribution at t=2 min with Ω=100 RPM in room-mid width

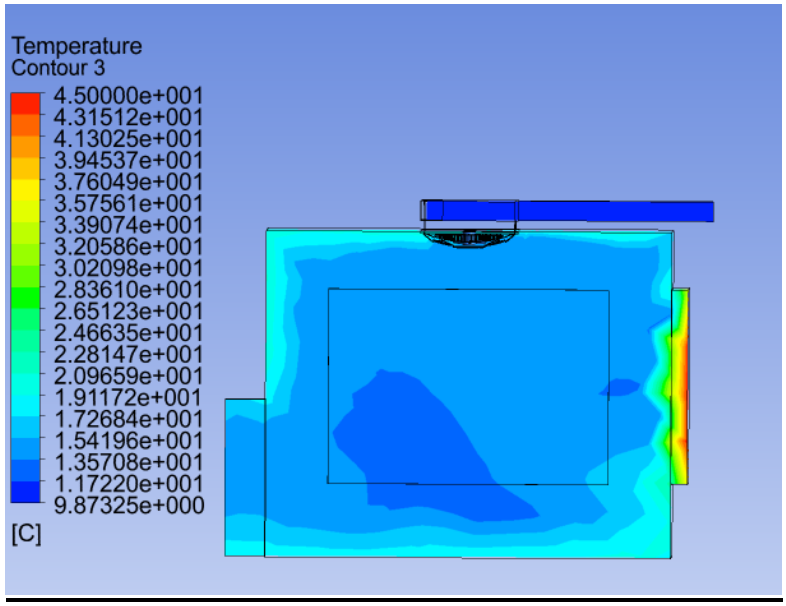

Figure (13) the flow temperature distribution at t=1 min with Ω=500 RPM in mid room width

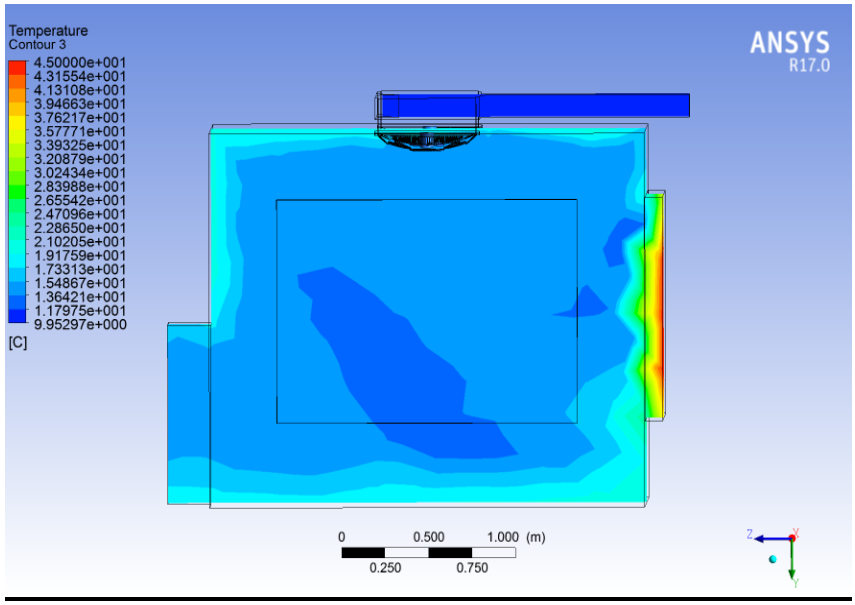

Figure (14) the flow temperature distribution at t=2 min with Ω=500 RPM in room-mid width

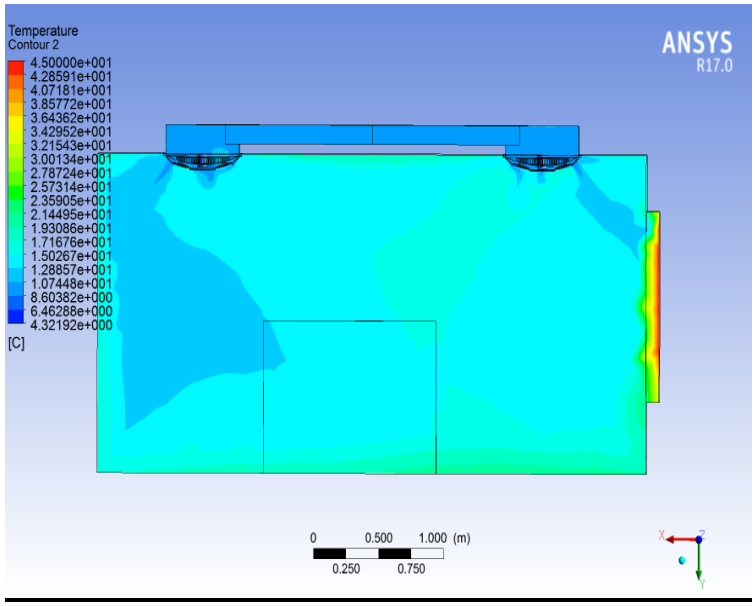

Figure (15) the flow temperature distribution at t=2 min with Ω=100 RPM in mid-room-length

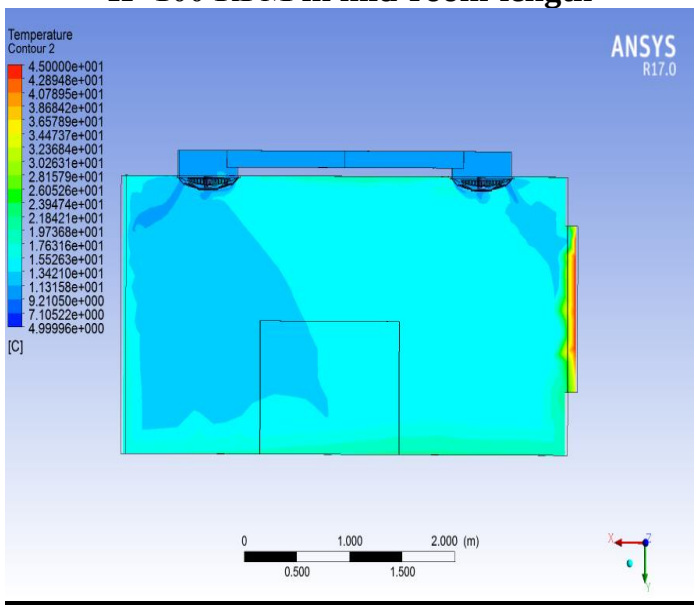

Figure (16) the flow temperature distribution at t=2 min with Ω=500 RPM in mid-room-length

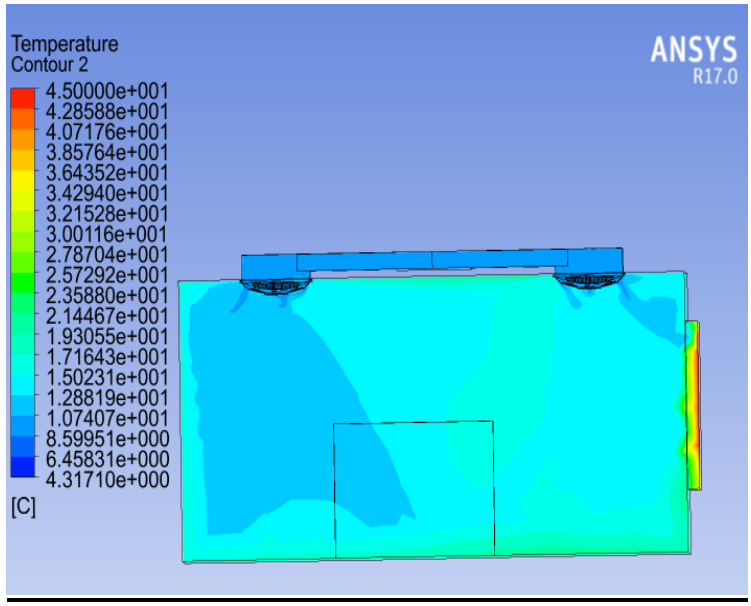

Figure (17) the flow temperature distribution at t=1 min with Ω=500 RPM in mid-room-length

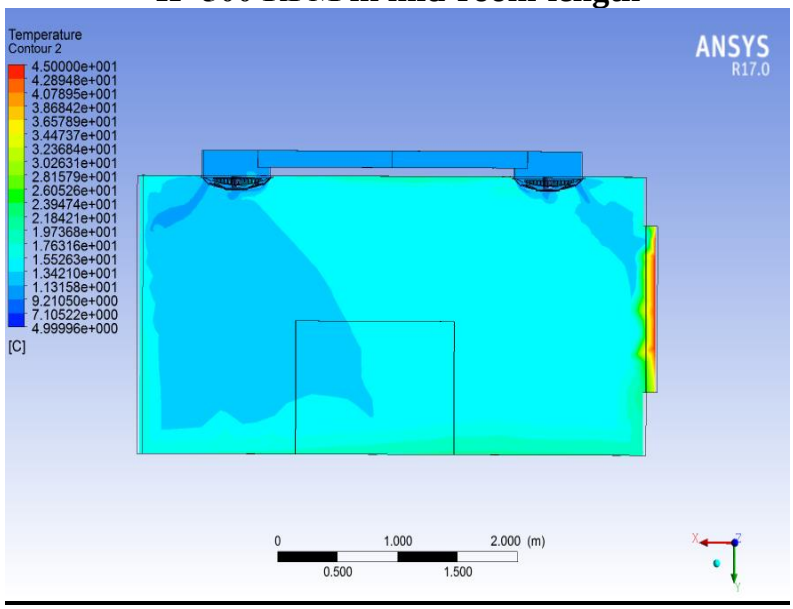

Figure (18) the flow temperature distribution at t=2 min with Ω=500 RPM

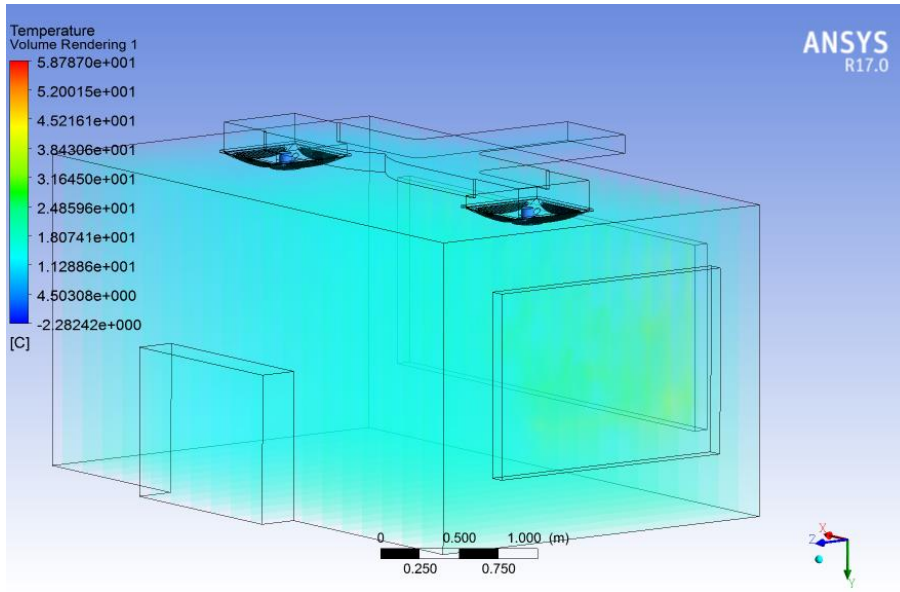

Figure (19) the entire room temperature distribution at t=1min with Ω=100 RPM

Appendix A
Nomenclature

Symbol	Definition
U	Linear velocity
P	Pressure
K	Kinetic energy of turbulence
Ω	Fan rotational velocity
μ	Fluid viscosity
Ɛ	Rate of dissipation of kinetic energy
ρ	Fluid density
C_1, C_2,σ_k,σ_ε	Turbulent model empirical constants
Ib	blackbody emission intensity
Iv	spectral emission intensity
r, s	position and directional vector
s	path length
Ka, Ks	absorption and scattering coefficients
V	frequency
T	local absolute temperature
Φ	in-scattering phase function
ω	solid angle
S	source term

الاستجابة الانتقالية لحيز هوائي مكيف معرض الى اشعاع شمسي ثابت

مصطفى احمد عبد الحسين
mustafa.ahmed1971@gmail.com
الجامعة التكنولوجية - قسم الهندسة الميكانيكية

المستخلص

تم عمل محاكاة لدراسة تأثير تغلغل الاشعاع الشمسي ذو كثافة ثابتة خلال نوافذ غرفة مكيفة على توزيع درجات الحرارة لغرفة ذات محتوى هوائي. تم تكييف الغرفة باستخدام مجرى مستطيل الشكل ذو تقسيمين حيث يتم توزيع الهواء باستخدام مروحتين سقفيتين من النوع الشبكي ذات سرعة متغيرة (100 و 500) دورة في الدقيقة. تمت عملية المحاكاة باستخدام برنامج ANSYS-CFX لجريان انتقالي خلال ازمنة محددة (1، 2 و 5) دقائق. اظهرت النتائج ان التغير في توزيع درجات الحرارة لزمن محدد مع تغير سرع المراوح ينعكس ايجابا على كفاءة التبريد للمحتوى الهوائي، ايضا لوحظ ان الاستجابة الانتقالية للمحتوى الهوائي نسبة للاشعاع الشمسي تكون موجودة بوضوح في المحاكاة مع ملاحظة تأثير المراوح في تسارع انتقال الحرارة خلال الحيز.

الكلمات الرئيسية: غرفة مكيفة، مراوح سقفية شبكية، اشعاع شمسي